JOC Article

Synthesis of (−)-(*R*)-Pyrrolam A and Studies on Its Stability: A Caveat on Computational Methods

Rhett T. Watson,† Vinayak K. Gore,† Kishan R. Chandupatla,† R. Karl Dieter,*,† and James P. Snyder*,‡

Department of Chemistry, Hunter Laboratory, Clemson University, Clemson, South Carolina 29634, and Department of Chemistry, Emory University, 1515 Dickey Drive, Atlanta, Georgia 30322

dieterr@clemson.edu; snyder@euch4e.chem.emory.edu

Received April 1, 2004

The asymmetric synthesis of (−)-(*R*)-pyrrolam A was achieved in three operations from *N*-Boc pyrrolidine via an α-(*N*-carbamoyl)alkylcuprate vinylation reaction followed by *N*-Boc deprotection and cyclization. One-pot deprotection−cyclization procedures led to mixtures of pyrrolam A and its double bond isomers. These isomerization events could be circumvented by use of a two-step procedure. To guide aspects of the experiments, a series of computational energy evaluations and chemical shift predictions were performed with molecular mechanics, semiempirical, ab initio, and density functional methods. The relative stabilities of the double bond isomers, as estimated by experiment, challenged a number of computational methods, and only the MP2 model with its moderate degree of electron correlation came close to matching the experimental data. The MP2 method was further applied to an unusual aspect of the double bond migration between pyrrolam A and its isomer **9**. The reaction (**1** to **9**) on neat samples is irreversible without racemization, and the alumina-mediated equilibration is accompanied by complete loss of enantiomeric excess. The source of the irreversibility was traced to asymmetric charge distribution in the intermediate dienolate anion. The analysis ultimately led to a semiquantitative sketch of the pyrrolam energy surface.

Introduction

The pyrrolizidine skeleton is found in many alkaloids isolated from plant extracts[1] and from insects[2] that feed upon the plants. These alkaloids and their metabolized products serve as pheromones and defensive agents in insect biology and display a range of biological activities in mammals.[3] Pyrrolams A−D (Figure 1, **1**−**4**) were isolated by Zeeck and co-workers in 1990 from the bacterial strain *Streptomyces olivaceus* (strain Tü 3082) by elution with methanol from Amberlite XAD-16 resin followed by further purification via column chromatography (silica gel, CH_2Cl_2/MeOH).[4] Bioassays revealed modest biological activity. Pyrrolam A was shown to have low herbicidal activity and to damage fertilized fish (*Brachydanio rerio*) eggs but was inactive against Gram-positive and Gram-negative bacteria, fungi, molds, viruses, worms, protozoa, and tumor cell lines.[4] Whereas pyrrolam A was isolated as a pure enantiomer, pyrrolams B−D were obtained as racemates. The chemical interconversion of pyrrolams A and C was considered unlikely, although the conversion of C to B was not ruled out.[4] Crystalline **1** experienced dimerization to **5** when allowed to stand in open vessels for extended periods of time. Since the initial isolation, pyrrolam A has been synthesized several times. Its conversion to pyrrolam C (**3**) has not been observed in these synthetic endeavors.[5−8] Carbinol amine **3** was nonetheless synthesized[9] prior to its reported isolation, and in one instance[9c] minor amounts of **1** were isolated as a byproduct.

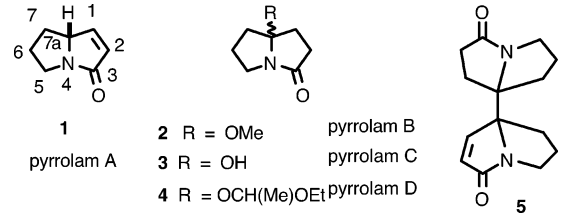

FIGURE 1. Pyrrolams A−D and dimer **5**.

† Clemson University.
‡ Emory University.

(1) (a) Wróbel, J. T. In *The Alkaloids: Chemistry and Pharmacology*; Brossi, A., Ed.; Academic Press: San Diego, 1985; Vol. 26, Chapter 7, p 327 and references therein. (b) Robins, D. J. *Fortschr. Chem. Org. Naturst.* **1982**, *41*, 115.
(2) Boppré, M. *Naturwissenschaften* **1986**, *73*, 17.
(3) Mattocks, A. R. *Chemistry and Toxicology of Pyrrolizidine Alkaloids*; Academic Press: London, 1986.
(4) Grote, R.; Zeeck, A.; Stümpfel, J.; Zähner, H. *Liebigs Ann. Chem.* **1990**, 525.
(5) Aoyagi, Y.; Manabe, T.; Ohta, A.; Kurihara, T.; Pang, G.-L.; Yuhara, T. *Tetrahedron* **1996**, *52*, 869.
(6) For syntheses of (*S*)-(+)-pyrrolam, A see: (a) Arisawa, M.; Takezawa, E.; Nishida, A.; Mori, M.; Nakagawa, M. *Synlett* **1997**, 1179 (b) Arisawa, M.; Takahashi, M.; Takezawa, E.; Yamaguchi, T.; Torisawa, Y.; Nishida, A.; Nakagawa, M. *Chem. Pharm. Bull.* **2000**, *48*, 1593. (c) Murray, A.; Proctor, G. R.; Murray, P. J. *Tetrahedron* **1996**, *52*, 3757.
(7) Giovenzana, G.; Sisti, M.; Palmisano, G. *Tetrahedron: Asymmetry* **1997**, *8*, 515.
(8) Huang, P. Q.; Chen, Q. F.; Chen, C. L.; Zhang, H. K. *Tetrahedron: Asymmetry* **1999**, *10*, 3827.

10.1021/jo049460r CCC: $27.50
Published on Web 08/05/2004

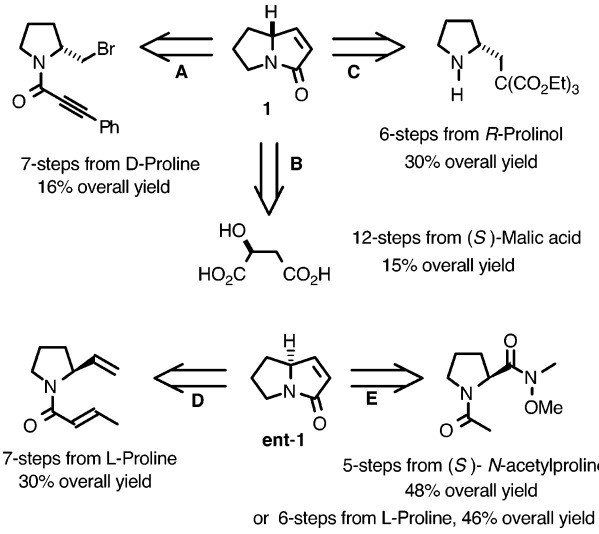

FIGURE 2. Asymmetric syntheses of (-)-(*R*)-pyrrolam A (**1**) and **ent-1**.

Asymmetric synthetic routes to pyrrolam A (**1**) and its enantiomer (**ent-1**) have all relied upon the chiral pool (Figure 2) for the pyrrolidine ring or for its construction. The first synthesis of **1** utilized expensive nonnatural D-proline (A)[5] and involved an intramolecular SmI_2-promoted cyclization, and a second approach from D-proline relied on intramolecular lactam formation (C).[7] The conversion of (*S*)-malic acid to **1** (B)[8] required the longest linear sequence but gave a reasonable overall yield. Naturally occurring L-proline was converted into **ent-1** via key cyclization steps involving either olefin metathesis (D)[6a−b] or Dieckmann cyclization (E).[6c] The low yield in the olefin metathesis reaction was attributed to the instability of the natural product under the reaction conditions. We now report a three-pot asymmetric synthesis of (*R*)-(−)-pyrrolam A. Observations from our synthetic endeavor suggest that pyrrolams B−C may well be artifacts of the isolation process arising from pyrrolam A via its $\Delta^{1,7a}$-isomer (i.e., **9**). The propensity for this double bond migration prompted computational studies on the relative stabilities of the two double bond isomers, which revealed an unusual combination of conjugation and strain effects that challenged a number of computational methods. Experimental verification of the most accurate calculations provides an assessment of the ability of various modeling procedures to handle strain and conjugation in small ring systems.

Results and Discussion

Synthesis. Pyrrolam A was readily synthesized in a three-pot sequence employing α-(*N*-carbamoyl)alkylcuprate methodology (Scheme 1).[10] Pyrrolidine amine protection gave *N*-Boc carbamate **6**, which was converted to a scalemic stereogenic organolithium reagent by asymmetric deprotonation[11] in Et_2O. Treatment of this organolithium reagent with a THF solution of CuCN·2LiCl at −78 °C afforded the scalemic stereogenic lithium dialkylcuprate reagent, which gave vinylation product **7** upon quenching with ethyl (*Z*)-3-iodopropenoate.[12] The reaction afforded excellent enantioselectivity on both a 1.0 mmol (95:5−96:4 er) and a 10 mmol scale (90:10 er). Deprotection and cyclization of **7** could be achieved in a single operation. Utilization of trifluoroacetic acid gave low yields of pyrrolam A (**1**), whereas good chemical yields could be obtained with either PhOH/Me_3SiCl[13] or trimethylsilyltriflate on a 1−2 mmol scale (Scheme 2, Table 1, entries 1, 2−3, and 5−6). Efforts to scale-up the one-pot *N*-Boc deprotection−cyclization protocol resulted in decreasing amounts of **1** and an increased yield of the $\Delta^{1,7a}$-enamide **9** (entries 3−4 and 6−7). The distribution of products **1** and **9** was a function of the experimental conditions (Scheme 2, Table 1). Attempted purification of the mixture of **1** and **9** via silica gel column chromatography (Scheme 2) gave pyrrolam A (**1**) and carbinol amide **3** (pyrrolam C). All efforts to cleanly effect the one-pot conversion of **7** to **1** proved unsuccessful. We therefore turned our attention to the HCl salt **8** (Scheme 2), which was readily prepared in quantitative yield from **7** with methanolic HCl (Me_3SiCl/MeOH). Initial efforts to neutralize **8** with various bases led to mixtures of bicyclic lactams **1**, **9**, **3**, and **10** (Scheme 2, Table 1).

Addition of a saturated aqueous $NaHCO_3$ solution to neat samples of **8** led to mixtures of pyrrolam A (**1**) and its double bond isomer **9** in various amounts depending upon the scale of the reaction (Table 1, entries 8−12). As the scale increased from 1 to 8 mmol, the ratio **1**:**9** changed from 88:12 to 71:29. Removal of solvent and exposure of the neat material to air, in one instance,

SCHEME 1

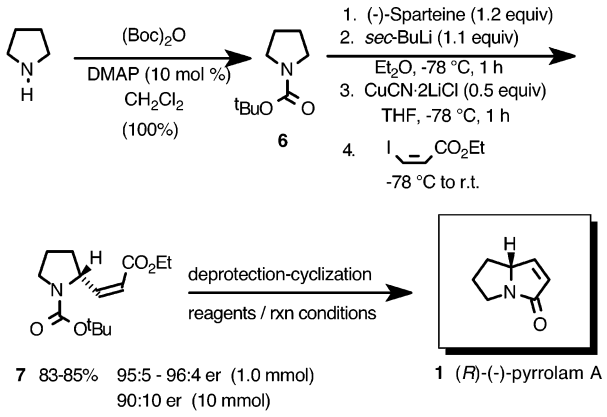

Reagents	Reaction conditions	% Yield	% ee
CF_3COOH (20%)	CH_2Cl_2, 25 °C, 12 h	20	
PhOH/Me_3SiCl (30/10 equiv)	CH_2Cl_2, 25 °C, 2 h	77-83	90
$Me_3SiOSO_2CF_3$ (1.2 equiv)	CH_2Cl_2, -40 to 25 °C, 12 h	64	90

(9) (a) Yoshifuji, S.; Arakawa, Y.; Nitta, Y. *Chem. Pharm. Bull.* ***1985***, *33*, 5042. (b) Ikeda, M.; Harada, S.; Yamasaki, A.; Kinouchi, K.; Ishibashi, H. *Heterocycles* **1988**, *27*, 943. (c) Flitsch, W.; Hampel, K. *Liebigs Ann. Chem.* **1988**, 387.

(10) For a review see: Dieter, R. K. Heteroatomcuprates and α-Heteroatomalkylcuprates in Organic Synthesis. In *Modern Organocopper Chemistry*; Krause, N., Ed.; John Wiley & Sons: New York, 2002; p 79.

(11) Beak, P.; Kerrick, S. T.; Wu, S.; Chu, J. *J. Am. Chem. Soc.* **1994**, *116*, 3231.

(12) (a) Dieter, R. K.; Topping, C. M.; Chandupatla, K. R.; Lu, K. *J. Am. Chem. Soc.* **2001**, *123*, 5132. (b) Dieter, R. K.; Oba, G.; Chandupatla, K. R.; Topping, C. M.; Lu, K.; Watson, R. T. *J. Org. Chem.* **2004**, *69*, 3076.

(13) (a) Kaiser, E., Sr.; Picart, F.; Kubiak, T.; Tam, J. P.; Merrifield, R. B. *J. Org. Chem.* **1993**, *58*, 5167. (b) Dieter, R. K.; Lu, K. *J. Org. Chem.* **2002**, *67*, 847.

TABLE 1. Distribution of Pyrrolam A (1) and Products Derived from It as a Function of Experimental Conditions

				products[a]			
entry	sample (mmol)	reaction conditions	product sample	**1**	**9**	**3**	**10**
1	**7** (1)	CF_3COOH, CH_2Cl_2		25	10[b]		
2	**7** (1)	PhOH, Me_3SiCl, CH_2Cl_2		50[c]	30		
3	**7** (2)			48[c]	40		
4	**7** (5)			20[a]	60[c]		
5	**7** (0.5)	TMSOTf, CH_2Cl_2		62[c]			
6	**7** (2)			70	30		
7	**7** (7)			20[c]	70[c]		
8	**8** (1)	aqueous $NaHCO_3$ (addition to **8**)		88	12		
9	**8** (3)			85	15		
10	**8** (5)			81	19		
11	**8** (5)			80	20		
12	**8** (8)			79	29		
13	**8**	aqueous $NaHCO_3$, **8** (THF suspension) inverse addition		60	30	10	
14	**8** (8)	Hexamethyldisilazane	**A**	66	33		
15	**8** (1)	LiHMDS (1.1 equiv), THF	**B**	10	90		
16	**8** (1)	LiHMDS (2.0 equiv), THF	**C**	1	99		
17	**A**	cold neat sample, standing 12 h	**D**	23	77		
18	**D**	(i) add Et_2O, filter ppt; (ii) Al_2O_3 purification	**E**	20	80		
19	**E**	$CDCl_3$ NMR sample, 12 h, 25 °C	**F**	20	80		
20	**F**	neat, open to air, solvent removal	**G**	14	16	13	57
21	**C**	purification on neutral alumina, EtOAc	**H**	20	80		
22	**C**	purification on basic alumina, EtOAc		28	21		51
23	**8**	aqueous $NaHCO_3$, CH_2Cl_2, inverse addition of **8**	**I**	100[d]	0		
24	**I**	neat, under Ar, refrigeration, 24 h	**J**	90[d]	10		
25	**J**	neat, under Ar, refrigeration, 48 h	**K**	85[d]	15		
26	**K**	neat, under Ar, refrigeration, 72 h	**L**	77[d]	23		
27	**L**	neat, under Ar, 25 °C, 96 h	**M**	51[d]	17	32	
28	**M**	$CDCl_3$ solution, refrigeration	**N**	55[d]		45	
29	**N**	(i) neutral alumina, EtOAc, Ar, 25 °C, 21 h; (ii) purification on silica gel (CH_2Cl_2/MeOH)	**O**[e]	8	18	54[c]	
30	**K**	purification on neutral alumina, EtOAc		25[f]	75		

[a] Determined from ^{1}H NMR ratios unless otherwise noted. [b] Monocyclic amines observed (approximately 35%). [c] Yields based upon isolated products purified by column chromatography. [d] Enantiomeric ratio = 90:10 as determined by chiral phase HPLC. [e] Dimer **5** was formed (20% molar ratio) as a 53:47 mixture of diastereomers. [f] Racemic as determined by chiral phase HPLC.

SCHEME 2

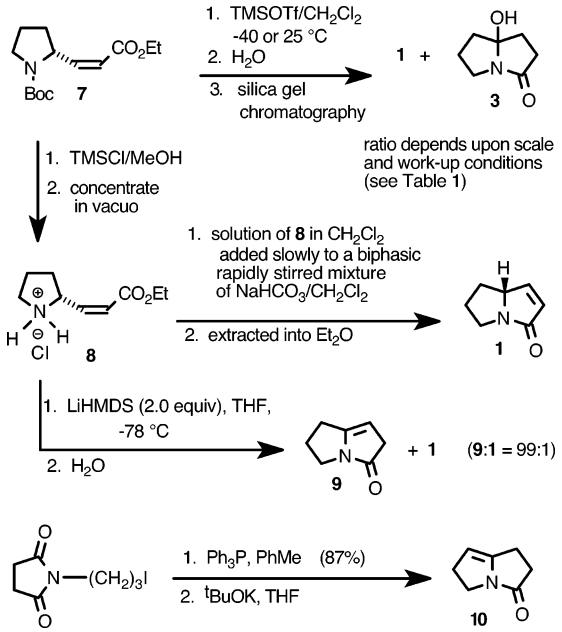

caused isomerization to **10** (57%) and capture of water to give carbinol **3** (13%) in addition to enamides **1** (14%) and **9** (16%) (Table 1, entry 20). Although this event was irreproducible, attempted purification of a mixture of **9**:**1** (99:1) on basic alumina gave **10**:**1**:**9** in a 51:28:21 ratio as determined by NMR analysis (entry 22). These two experiments gave a 78:22 and a 71:29 ratio of **10**:**9**, respectively, indicating the greater stability of **10** relative to **9**. Although **10** has been reported in the literature,[9c,14] no spectral data is available, and we were unable to separate **9** and **10** by silica gel or alumina chromatography. Nonetheless, GC−MS analysis of a mixture of **1**:**9**:**10** (determined by NMR analysis) showed two separate ion-current peaks, each of which displayed a similar mass spectrum indicative of isomers. The ^{1}H and ^{13}C NMR absorptions due to **1**, **3**, or **9** could be identified from the NMR spectra of pure samples of **1**, **3**, or **9**. The remaining absorptions attributed to **10** include a triplet (δ 4.59, calcd 5.4) in the ^{1}H NMR spectrum for an enamide olefin proton. ^{13}C absorptions at δ 97.4 and 147.2 were assigned to the enamide double bond, and that at δ 170.9 corresponds to the amide carbonyl. To more fully characterize **10**, we performed a series of calculations to predict the NMR chemical shifts for the compound. Figure 3 includes results for the latter and a comparison with compounds **1** and **9** as standards. It can be seen that density functional (mPW1PW91[15,16]/6-311G*//Becke3LYP/6-311G*) and fragment database (ACD)[17] evaluations readily assign the spectrum for **1** and **9** and equally accurately account for the ^{1}H and ^{13}C spectra for structure **10**. Although the quantum chemical approach is more faithful to experiment, both methodologies leave little doubt

(14) Ha, D.-C.; Yun, C.-S.; Yu, E. *Tetrahedron Lett.* **1996**, *37*, 2577.
(15) Adamo, C.; Barone, V. *J. Chem. Phys.* **1998**, *108*, 664−675.
(16) Cimino, P.; Gomez-Paloma, L.; Duca, D.; Riccio, R.; Bifulco, G. *Magn. Res. Chem.* **2004**, in press.
(17) The Advanced Chemistry Development (ACD) Labs CNMR Predictor [http://www.acdlabs.com/].

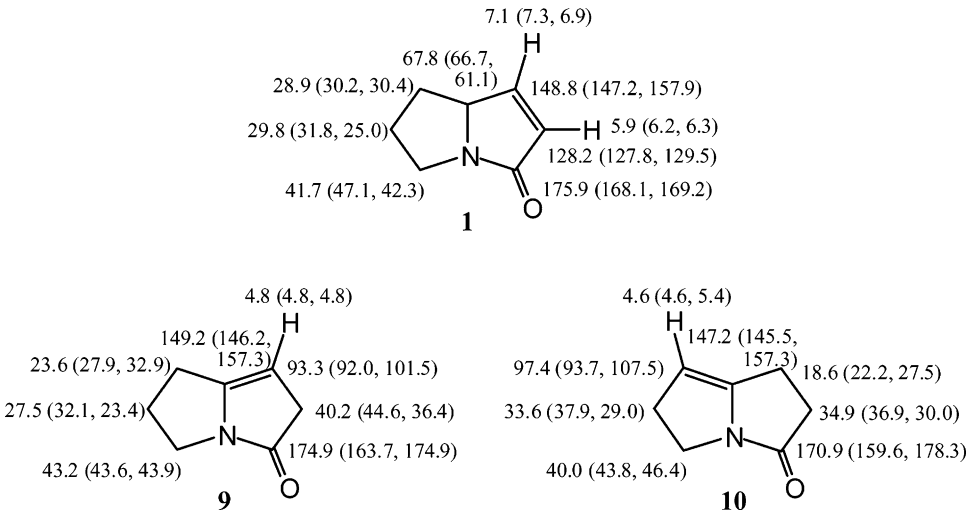

FIGURE 3. Comparison of ^{1}H and ^{13}C NMR chemical shifts for pyrrolam isomers **1**, **9**, and **10** (ppm relative to TMS). The first value is experimental, the second parenthetical value is mPW1PW91/6-31G*//Becke3LYP/6-311G*, and the third is the ACD database fragment prediction.

as to the location of the double bond. A comparison of several quantum chemical methods for calculating ^{13}C chemical shifts in the present series is discussed in Molecular Modeling below. Subsequently, enamide **10** was synthesized via an intramolecular Wittig reaction (Scheme 2) affording ^{13}C NMR absorptions identical to those abstracted from the spectrum for the mixture of **1**:**9**:**10** and to those calculated (Figure 3).

Neutralization of **8** with hexamethyldisilazane afforded **1** and **9** in a 66:33 (Table 1, entry 14) ratio. Manipulation of this material (i.e., A) during NMR sample preparation and recovery resulted in isomerization of **1** to **9** to afford a **1**:**9** ratio of roughly 1:4 (entries 17−19), indicating greater thermodynamic stability for enamide **9**. Attempted neutralization of **8** with aqueous sodium methoxide gave an intractable mixture by TLC analysis (20 spots). Neutralization of **8** with lithium hexamethyldisilazide afforded largely enamide **9** (entries 15 and 16) with small amounts of **1** obtained when a slight excess of LHMDS was employed and only a trace of **1** when 2 equiv of LHMDS were used. In general, the mixtures rich in **1** range from a ratio of 7.3:1 (entry 8) to 2:1 (entries 13 and 14) for an energy spread of $\Delta G^{298} = 0.4-1.2$ kcal/mol. Those rich in **9** range from a ratio of 99:1 (entry 16) to 1:1 (entry 20) for a similar inverse energy spread of −0.1 to −2.7 kcal/mol. Entry 20 furthermore suggests a **10**/**1** ratio of 4:1.

Attempted purification of **9** (**1**:**9** = 1:99) by neutral alumina flash column chromatography gave a 20:80 mixture of **1**:**9**, and attempted purification of a mixture of **9**:**1** (99:1) on basic alumina gave **10**:**1**:**9** in a 51:28:21 ratio (Table 1, entries 21−22). Although we were unable to achieve careful equilibration between, **1**, **9**, and **10**, the relative stability of these double bond isomers appears to be in the order of **10** > **9** > **1** with the **9**:**1** stability difference reflected in an 80:20 ratio and the **10**:**9** stability difference represented by ratios of 71:29 to 78:22. Averaging leads to an approximate **10**:**9**:**1** ratio of 12:4:1 (i.e., 69%, 25%, and 6%). At 25 °C these distributions correspond to ΔG^{298} values of 0.0, 0.6, and 1.4 kcal/mol, respectively. All efforts to effect equilibration between **1**, **9**, and **10** under acid catalysis (e.g., *p*-TsOH/CH_2Cl_2, pyrridinium *p*-toluenesulfononate/CH_2Cl_2, etc.) resulted in decomposition of the material and formation of additional products as evidenced by analytical TLC.

Although insoluble in THF, addition of a suspension of **8** in THF dropwise to a cold rapidly stirring biphasic mixture of CH_2Cl_2 and an aqueous $NaHCO_3$ solution gave rise to **1** and **9** (60:30) along with minor amounts of **3** (Table 1, entry 13). Dissolution of **8** in dichloromethane followed by dropwise addition to a cold rapidly stirring biphasic mixture of methylene chloride and aqueous $NaHCO_3$ gave clean pyrrolam A uncontaminated with its double bond isomers (entry 23). This procedure was reproducible and on a 3 mmol scale gave excellent yields (90%) of pyrrolam A with 90:10 er as measured by chiral stationary phase HPLC on a CHIRALCEL OD column [cellulose tris(3,5-dimethylphenylcarbamate) on silica gel]. An NMR sample of this material (i.e., **1**) in $CDCl_3$ did not undergo isomerization to **9** when stored in the refrigerator for 96 h. A neat sample of crude **1** stored in a round-bottom flask in the refrigerator slowly isomerized to **9**. ^{1}H NMR and chiral stationary phase HPLC measurements at 24 h [**1**:**9** = 90:10, er = 90:10], 48 h [**1**:**9** = 85:15, er = 90:10], and 72 h [**1**:**9** = 77:23, er = 90:10] revealed that isomerization of **1** to **9** occurred without racemization of the remaining **1**, ruling out an equilibrium process (Table 1, entries 23−26). Eventual inadvertent addition of water to the sample led to formation of **3** (entry 27) and eventually to a mixture of **1** and **3** (entry 28). Exposure of this sample to EtOAc/neutral alumina for 21 h led to formation of dimer **5** as a 53:47 mixture of diastereomers [a set of doublets at δ 7.02 and 6.05 and a second set at δ 6.82 and 5.85 with $J = 6.0$ Hz] (entry 29). Interestingly, the isolation study reported the formation of **5** as a single diastereomer [δ 7.08 (d, $J = 5.8$ Hz, 1H) and 6.06 (d, $J = 5.8$ Hz, 1H)] when **1** was allowed to stand neat for 3 weeks in an open vessel.[4] Purification of the NMR sample (32 mg) by silica gel column chromatography [MeOH/$CHCl_3$ (1:9, v/v)] gave a white solid whose melting point and specific rotation were

TABLE 2. Experimental and Calculated Relative Energy Differences between Double Bond Isomers 1, 9, and 10[a]

method	1	9	10
experimental	0.8 (21)	0.0 (79)	
Beck3LYP/6-311G*	3.6 (0.2)	0.7 (23.4)	0.0 (76.4)
MP2/6-311G*	0.8 (15)	0.0 (56)	0.4 (29)
MP2/6-311+G*	0.0(52)	0.3(32)	0.7(16)
MM3* (gas)	0.0 (91)	1.4 (9)	4.1 (0.1)
($CHCl_3$)	0.0 (96)	1.9 (4)	4.5 (0.05)
(H_2O)	0.0 (96)	1.9 (4)	4.0 (0.1)
MMFF (gas)[b]	0.0 (100)	32.5 (0.0)	24.0 (0.0)
($CHCl_3$)	0.0 (100)	33.3 (0.0)	24.7 (0.0)
(H_2O)	0.0 (100)	34.3 (0.0)	25.3 (0.0)
Sybyl[c]	0.0 (100)	4.5 (0.0)	15.9 (0.0)
Sybyl[d]	2.5 (1)	0.0 (90)	1.4 (9)
AM1[d] (gas)	3.3 (0.2)	0.2 (41.8)	0.0 (58)
(H_2O)[e]	3.1 (0.4)	0.5 (30)	0.0 (69.6)
PM3[d] (gas)	3.3 (0.3)	0.0 (81.7)	0.9 (18)
(H_2O)[e]	2.1 (3)	0.0 (86)	1.2 (11)
MNDO[d] (gas)	8.4 (0.0)	0.1 (46)	0.0 (54)
(H_2O)[e]	7.4 (0.0)	0.4 (34)	0.0 (66)

[a] Calculated populations at 298 K are given in parentheses, kcal/mol. [b] A nearly identical result is obtained from MMFF in MacSpartan-02 and Spartan-04.[27] [c] MacSpartan, Tripos force field. [d] Spartan-04, Tripos force field. [e] SM5.4/p[23] as implemented in Spartan-04.

close [26.5 mg, mp 56−58 °C, $[\alpha]_D$ −21.7 (c = 1.06, $CHCl_3$)] to those reported for the natural product.[4] Thus, conditions are available for the preparation of pyrrolam A on a large scale.

MP2 Evaluation of the Pyrrolam Isomer Energy Surface. Our goals in applying modeling to the pyrrolam problem were 3-fold. First, given the variability of product composition and ratios listed in Table 1, we sought an accurate assessment of the relative energies for **1**, **9** and **10** independent of the estimates from the tabulated mixtures. Second, while we initially anticipated that tautomeric exchange among the latter compounds could be described in terms of a straightforward equilibrium process, the rearrangement of neat **1** to **9** without racemization and the infrequent appearance of **10** in the mixtures suggested otherwise. Consequently, in an attempt to understand the pyrrolam isomer potential energy surface, we examined the possible role of the base-promoted anionic intermediates **13** and **14** (Scheme 4 and Figure 6). Third, the literature has been unclear on the possibility of forming pyrrolam C (**3**) from the A form (**1**) in contrast to its being a functional component of the natural product isolate. We felt that evaluation of the consequences of acid-promoted formation of an intermediate cation would assist interpretation of the experimental outcomes. Although a variety of methods were used to estimate relative energies for the pyrrolam tautomers (Table 2), the most reliable protocols involved optimizing molecular geometries with density functional theory and a triple-ζ basis set (Becke3LYP/6-311G*) in some cases augmented with a diffuse function (Becke-3LYP/6-311+G*) followed by energy evaluation with MP2 at the same level. Thus, energies and electronic properties were derived by MP2/6-311G*//Becke3LYP/6-311G* and MP2/6-311+G*//Becke3LYP/6-311+G*.[18] The diffuse (i.e., "+") function was included to accommodate the negatively charged intermediates **13** and **14**.

(18) *Gaussian 03*, Revision A.1; Frisch, M. J. et al.; Gaussian, Inc.: Pittsburgh, PA, 2003.

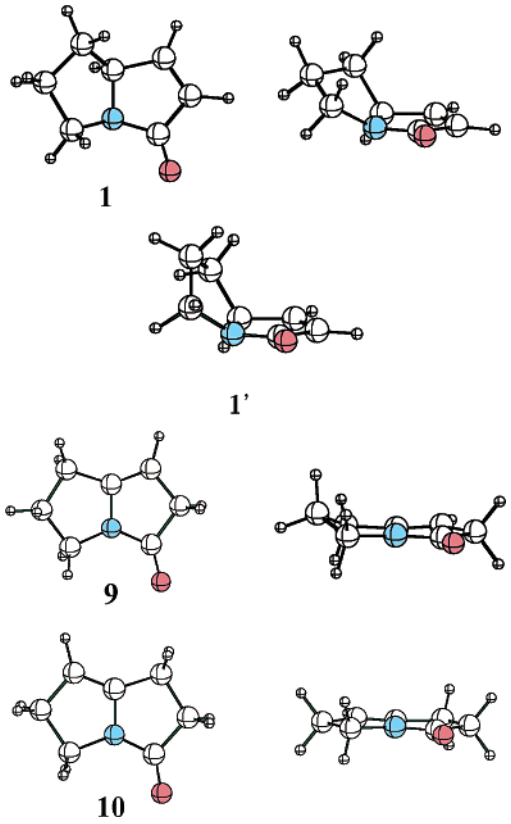

FIGURE 4. Geometries of the density functional Becke3LYP/6-311+G*//Becke3LYP/6-311+G* optimized conformations of **1**, **9**, and **10**, top and side views. Pyrrolam **1** exists in two conformations, **1** and **1′**.

Pyrrolam Isomer Relative Energies. Table 1 illustrates that the ratio of **1**:**9** formed depends on the reaction microenvironment but that both acid and base conditions lead to mixtures. Analysis of the tabulated experiments above led us to conclude that the stability order is most likely **10** > **9** > **1** with a ΔG^{298} energy spread of 0.0, 0.6, and 1.4 kcal/mol (i.e., 12:4:1), respectively. Clearly, the three isomers are similar in energy. The MP2/6-311+G*//Becke3LYP/6-311+G* level predicts the dominant isomer at room temperature to be **1** (52% population; 0.0 kcal/mol) with **9** and **10** appearing in smaller but observable amounts (32% and 16% populations, ΔE_{rel} = 0.3 and 0.7 kcal/mol, respectively). The corresponding **10**:**9**:**1** ratio of 1:2:3.3 is to be compared to the Table 1 analysis estimate of 12:4:1. The source of this discrepancy is not apparent, though it could lie in the fact that thermodynamic equilibration has not been achieved in the isomerization reactions or with inaccuracies in the MP2 relative energies. Recalculation of the latter with a solvent correction (polarizable continuum model (PCM)[19]) at a dielectric constant of 6.89 (ethyl acetate, ϵ = 6.02) gave nearly identical energy differences. The major point of agreement is that energy differences in both estimates fall within the rather narrow 1.4 kcal/mol window. Structurally, compound **1** exists as a folded structure in two conformations (Figure 4). The chairlike

(19) (a) Cancès, M. T.; Mennucci, B.; Tomasi, J. *J. Chem. Phys.* **1997**, *107*, 3032. (b) Cossi, M.; Barone, V.; Mennucci, B.; Tomasi, J. *Chem. Phys. Lett.* **1996**, *286*, 253. (c) Cossi, M.; Scalmani, G.; Rega, N.; Barone, V. *J. Chem. Phys.* **2002**, *117*, 43.

SCHEME 3. $\Delta^{5,6}$- (11) and $\Delta^{6,7}$(12)-Double Bond Isomers of Pyrrolam A

form is more stable than the boat form **1′** by 1.1 kcal/mol. Isomer **9** is nearly flat but sustains a slight envelope shape in the saturated five-membered ring. Compound **10** is completely planar.

All efforts to effect controlled acid-catalyzed interconversion of **1** and **9** or equilibration between **1**, **9**, and **10** led to complex mixtures of numerous products as evidenced by TLC analysis. The identities of the minor components in these complex mixtures were not established. In two instances (neat sample left standing, treatment with basic alumina; Table 1, entries 20 and 22), putative enamide **10** was obtained as the major component of the mixture. There are, of course, two other double bond isomers within the pyrrolam family, namely, **11**[20] and **12**[21] (Scheme 3), both of which are known compounds. At the MP2/6-311G*//Becke3LYP/6-311G* and MP2/6-311+G*//Becke3LYP/6-311G* levels we calculate the energies relative to global minimum **1** to be 2.2 and 2.3 kcal/mol, respectively. At 25 °C these values would correspond to populations of 1.2% and 1.0%, respectively. If the calculations closely represent the equilibration experiments, these compounds could be present in small quantities as components of the complex mixture of products. We have not, however, observed **11** or **12** in the mixtures.

Racemization-Free Rearrangement of 1 to 9. Subsequent experiments with pyrrolam samples enriched in **1** (i.e., **9**:**1** = 15:85) and **9** (i.e., **9**:**1** = 99:1) led to nearly identical 75:25 and 80:20 mixtures of **9**:**1**, respectively, when either sample was subjected to column chromatography on alumina with EtOAc at room temperature (Table 1, entries 21 and 30). Accordingly, one is led to postulate that the 75:25 to 80:20 value represents the mixture at thermodynamic equilibrium under these conditions. The striking observation that the neat rearrangement of **1** to **9** proceeds with a constant er of 90:10 for **1** suggests that equilibrium concentrations are approached without equilibrium. The implication is that transformation of chiral **1** to achiral **9** is irreversible and that thermodynamic conditions are not achieved. One interpretation of the results assumes that isomerization proceeds through the highly delocalized and planar anion **13** (Scheme 4).

The electronic characteristics of **13** at the MP2/6-311+G* level of theory as expressed by natural bond orbital (NBO) analysis[22] are depicted in Figure 5a. The Wiberg bond orders reveal two interesting features. First, the π-bond with the greatest degree of double bond

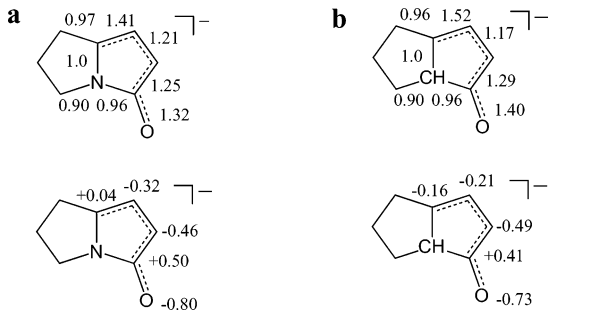

FIGURE 5. Selected MP2/6-311+G* NBO bond orders and atomic charges for intermediate anion **13** (a) and the corresponding carbon analogue (b) geometry optimized with the DFT Becke3LYP/6-311+G* model.

SCHEME 4

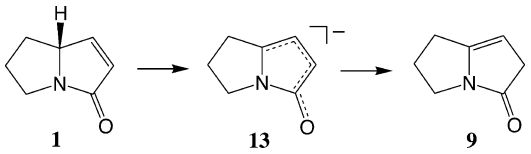

SCHEME 5

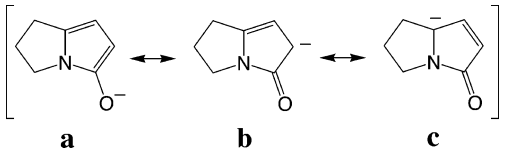

character is found between C-1 and C-7a (i.e., NC_{7a}-C_1). Second, the three bonds to nitrogen are all single, implying that the π-type lone electron pair on N has been essentially isolated from the delocalized anion except for its repulsive character. In resonance theory terms, the relative contribution of the structures is thereby predicted to be in the order a > b > c (Scheme 5) with no significant contribution from amide resonance.

The NBO charge distribution (Figure 5a) is in line with this view but adds an additional insight. Whereas sizable negative charge is located at carbon α to the carbonyl (-0.46), the γ carbon is neutral or even slightly positive ($+0.04$). Thus, nitrogen adjacent to C-γ not only repels electrons through the π-framework but withdraws them through the N$-$C σ-bond framework as well. Consequently, once a proton is removed from **1** to give **13**, reprotonation is predicted to take place exclusively at O or C-α in the neat reaction. If this view is accurate, then the corresponding all-carbon anion would be expected to possess electronic properties more conducive to protonation at both α- and γ-carbons. Indeed, the calculations displayed in Figure 5b illustrate negative charge at both centers albeit polarized by the conjugated carbonyl.

Rearrangement of 9 to 1. We speculated that under conditions where achiral **9** rearranges to **1**, reprotonation should occur from both faces of planar anion **13** leading to racemization. This hypothesis was tested with a mixture of approximately 15:85 for **9**:**1** and a 90:10 er for **1**. The blend was chromatographed on an Al_2O_3 column in EtOAc to give a 75:25 mixture of **9**:**1** with an er of 0. The latter result demonstrates that both **1** and **9** are deprotonated and confirms the predicted racemization. In addition, the 75:25 ratio is a close match of the

(20) Thomas, E. W.; Rynbrandt, R. H.; Zimmermann, D. C.; Bell, L. T.; Muchmore, C. R.; Yankee, E. W. *J. Org. Chem.* **1989**, *54*, 4535.

(21) (a) Martin, S. F.; Chen, H.-J.; Courtney, A. K.; Liao, Y.; Pätzel, M.; Ramser, M. N.; Wagman, A. S. *Tetrahedron* **1996**, *52*, 7251. (b) Andersson, P. G.; Bäckvall, J. E. *J. Am. Chem. Soc.* **1992**, *114*, 8696.

(22) (a) Reed, A. E.; Curtiss, L. A.; Weinhold, F. *Chem. Rev.* **1988**, *88*, 899−926. (b) Weinhold, F. Natural Bond Orbital Methods. In *Encyclopedia of Computational Chemistry*; Schleyer, P. v.R., Allinger, N. L., Clark, T., Gasteiger, J., Kollman, P. A., Schaefer, H. F., III, Schreiner, P. R., Eds.; John Wiley & Sons: Chichester, UK, 1998; Vol. 3, pp 1792−1811. (c) cf. http://www.chem.wisc.edu/~nbo5/index.htm.

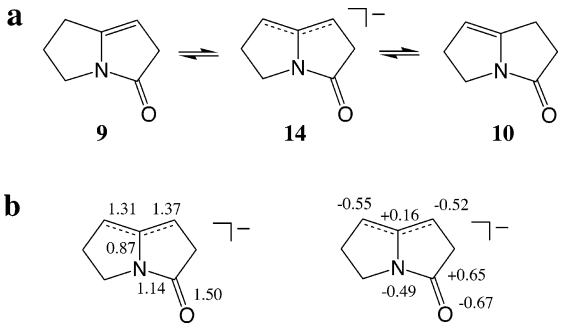

FIGURE 6. (a) Anion **14** connecting pyrrolam isomers **9** and **10**; (b) selected MP2/6-311+G* NBO bond orders and atomic charges for **14**.

80:20 proportion derived from the 99:1 sample of the two isomers described above as an equilibrium value.

Elusiveness of 10 and the Pyrrolam Energy Surface. Table 1 reveals that pyrrolam **10** rarely appears under conditions where **1** and **9** can be interconverted. Given that all three isomers are calculated to lie within 0.7 kcal/mol of one another (see above), this result is surprising. Accordingly, we optimized the geometry of anion **14** (Figure 6a), the putative intermediate that connects **9** and **10**. Anion **14** is characterized by approximate symmetry around the allylic fragment both in terms of bond orders and atomic charges (Figure 6b). The system can be expected to protonate readily at either of the allylic carbons, facilitating a true equilibrium between **9** and **10**. Unlike anion **13**, **14** shows the classical amide resonance as indicated by the enhanced and reduced N−C(=O) and C=O bond orders, respectively. Structure **14** with its planarity and 6-π electrons located around the bridgehead is a candidate for Y-aromatic character.[23] However, the calculated single bond order for the bridging N−C bond makes it clear that nitrogen experiences little productive interaction with the essentially π-isolated all-carbon allylic anion center.

In the two instances of the appearance of compound **10** in mixtures reported above, one of which involved exposure to basic alumina, both **1** and **9** were likewise present in near 1:1 ratios to the extent of 25−50% of **10**. This is consistent with the notion that under conditions sufficient to produce the latter, the other isomers are generated and interconverted as well. Assuming a base-catalyzed process, this requires formation of both anions **13** and **14**, the latter of which is predicted to be less stable than the former by 19.9 kcal/mol (MP2/6-311+G*). The considerable energy gap can be attributed to differences in conjugation, strain, and internal electron repulsion. Importantly, it explains the only occasional appearance of **10** from the multitude of acid−base experiments carried out to form the pyrrolam structure (Table 1). It would appear that rather strong basic conditions are required to strip the proton from C-7 in **9** to generate anion **14**. Once formed, however, the intermediate most certainly resides in an environment energetically sufficient to deliver all three double bond isomers.

The experimental observations and accompanying calculations permit a rough sketch of the energy relationships in the pyrrolam system. Figure 7 provides the graphic. Isomers **1**, **9**, and **10** are within 1 kcal/mol of one another. Enol **15**, not observed in the present work, lies 13 kcal/mol above **1**, and dienolate **13** is 20 kcal/mol more stable than allyl anion **14**. The irreversible and racemization-free rearrangement of **1** to **9** is captured by the intersecting dotted lines representing two transition states of unspecified energies bracketing **13**. These indicate a strong kinetic preference for proton capture by **13** to give achiral **9** or enol **15**. We do not suggest that **15** is an obligatory intermediate on the path to **9**, only that the bias for protonating either C-2 or O versus C-7a in **13** is highly favored (cf. Figure 5). Excessive quantities of **9** in the presence of base (Al_2O_3) lead irreversibly to the 80:20 ratio of **9**:**1**, an approximation to thermodynamic equilibrium. On the other hand, excessive quantities of **1** under similar conditions generate a comparable 75:25 ratio, this time establishing a true equilibrium.

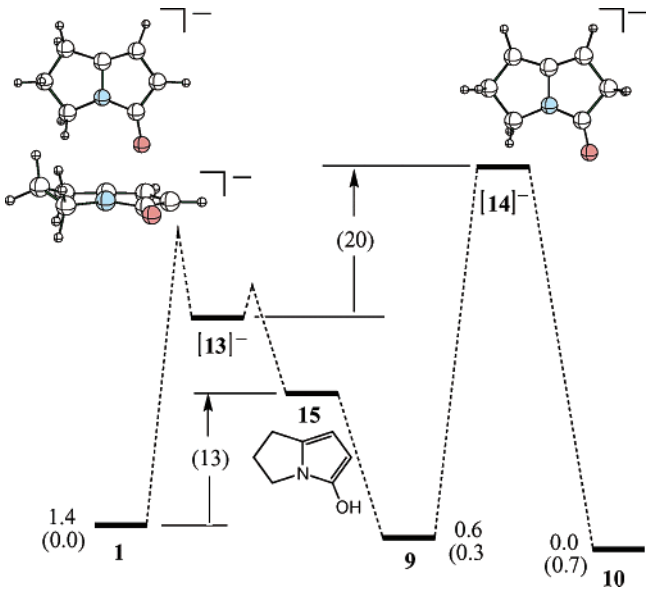

FIGURE 7. Pyrrolam energy relationships based on a combination of experiment and MP2/6-311+G*//Becke3LYP/6-311+G* energies (kcal/mol), calculated energies in parentheses. Slightly nonplanar anion **13** (pictured upper left) is surrounded by two transition states, the lower energy one leading directly to either **9** or **15** or both. Anion **14** (upper right) is planar.

Pyrrolam Capture of Nucleophiles. Nucleophilic capture during preparation of **1** and **9** most certainly involves ammonium cation **16**. Such a species is an obvious intermediate to both the oxygenated substances **2**, **3**, and **4** and the dimer **5**. To develop a perspective on the ability of **16** to divert the neutral pyrrolam species by nucleophile capture, we have constructed the reactions of Scheme 6 at the MP2/6-311G*//Becke3LYP/6-311G* level.

With the hydronium ion as the general acid proton donor in eq 1, the reaction is strongly exothermic. Capture of a water molecule leading to carbinol **3** is estimated to be uphill in energy by 26.7 kcal/mol. The overall result of hydrating enamide **9** to **3** corresponds to an energy drop of 26.1 kcal/mol at the MP2 level. In the context of equilibrating pyrrolam isomers, which differ in energy by no more than 2−3 kcal/mol by the same method, if **16** is a genuine intermediate, its interac-

(23) Gobbi, A.; MacDougall, P. J.; Frenking, G. *Ang. Chem. Int. Ed. Engl.* **1991**, *103*, 1001−1003. (b) Skancke, A. *J. Phys. Chem.* **1994**, *98*, 5234−5239.

SCHEME 6

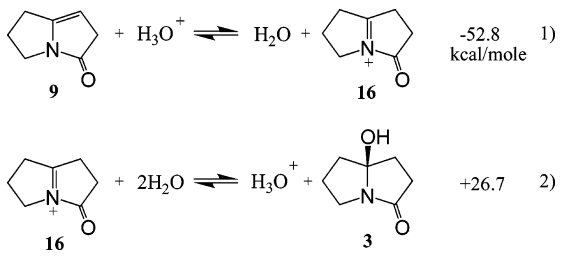

SCHEME 7

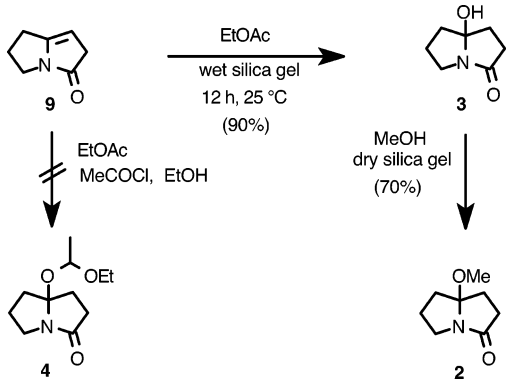

tion with an oxygen-containing nucleophile in the presence of acid is predicted to be highly favored. To test this idea we treated **9** separately with MeOH, H_2O, or EtOAc under acidic conditions, and in all instances obtained a complex mixture of products. However, treatment of **9** dissolved in ethyl acetate with wet silica gel cleanly afforded **3** in high yield, which in turn could be converted to **2** by treatment with methanol and dry silica gel (Scheme 7). Although the formation of **4** was not achieved, these observations strongly suggest that pyrrolams B−D are artifacts of the isolation procedure and not organism metabolites.

Molecular Modeling. Prior to determination of the identity and ratio of products from the experiments reported in Table 1, we attempted to evaluate the relative stabilities of pyrrolam isomers with various molecular mechanics and semiempirical quantum chemical methods. The results were uneven and contradictory (Table 2). With one exception, all the force field variations in MacroModel and different versions of Spartan delivered structure **1** as the global minimum with virtually no contribution from **9** or **10**. Application of the continuum solvation model had little impact on this outcome. The MMFF method was particularly unfaithful to experiment, suggesting abnormally high energies for the latter two isomers. It is clear that the MMFF force field parameters for the fused and unsaturated five-membered rings apply unevenly across the range of double bond isomers. An older version of Sybyl molecular mechanics accurately predicts **9** to be the most stable species but seriously underestimates the relative proportion of **1**.

The semiempircal methods all predict **9** to be low in energy and of somewhat comparable stability to **10**. However, the same methodology significantly underestimates the stability of **1**. The results are not altered by including the SM5.4 aqueous solvation model of Hawkins, Cramer, and Truhlar.[24] In this respect, the Becke3LYP density functional approach even with a triple-ζ basis including polarization (6-311G*) is insufficient to improve the energy of **1** relative to **9** so as to model the experimental equilibrium ratio of **9**:**1**, i.e., 80:20. It would appear that the present pyrrolam series (**1**, **9**, and **10**) presents a particularly challenging relative energy estimation problem for the methods routinely applied in synthetic chemistry. For the peculiar blend of delocalization and strain across the trio of double-bond isomers, the relative energetics is poorly handled by all parametric methods and by a rather robust density functional approach as well. Only the MP2 model, with its capacity for a moderate degree of electron correlation, comes close to matching the experimental data in terms of predicting relative energies and populations. Even here, the question of the relative energy of **10** remains an open question. It might be possible to resolve this experimentally by seeking more controlled conditions that allow the range of isomers to be fully equilibrated. Similarly, higher levels of theory that expand the basis set and include additional layers of electron correlation would provide additional confidence in the MP2 estimates for **1**, **9**, and **10**. We see these issues as the subject of attention in a future report.

With respect to the ^{13}C and ^{1}H chemical shift calculations, we employed single point ab initio (RHF and MP2) and density functional (Becke3LYP and mPW1PW91) methodologies with 6-31G* and 6-311G* basis sets applied to Becke3LYP/6-311G* optimized geometries for **1**, **9** and **10**. Table S-1 (Supporting Information) illustrates that the MP2/6-311G* and mPW1PW91/6-31G* approaches provide superior agreement with experiment and are comparable in accuracy. However, the MP2 calculations require much more computer memory (see Experimental Section) and are approximately 20 times slower. As a result the density functional method is preferred for molecules in the size range of natural products and drug-like molecules.[16]

Summary and Conclusions

In summary, the rapid three-pot asymmetric synthesis of (*R*)-(−)-pyrrolam A illustrates the synthetic potential of scalemic stereogenic α-(*N*-carbamoyl)alkylcuprates for the synthesis of enantiopure alkaloids. Conditions for avoiding the isomerization of pyrrolam A (**1**) to enamide **9** have been developed, permitting the larger scale synthesis of the natural product. A surprising result is the observation that a neat sample of a 90:10 mixture of **1**:**9** with an er of 90:10 for chiral **1** underwent isomerization in the cold *without* racemization. The process was judged to be irreversible and kinetically controlled. NBO analysis with the MP2/6-311+G* model reveals a highly asymmetric charge distribution at C-2 and C-7a for the dienolate anion **13**. The corresponding negative and neutral/positive atomic charges, respectively, appear to lead to exclusive proton capture at C-2 to give **9**. A parallel set of experiments on a 15:85 mixture of **9**:**1** (er of 90:10 for **1**) treated to chromatography over alumina led to a 75:25 equilibrium mixture *with* racemization. Further geometry optimization using density functional theory followed by MP2 energy evaluation (MP2/6-311+G*//Becke3LYP/6-311+G*) allowed the construction

(24) Hawkins, G. D.; Cramer, C. J.; Truhlar, D. G. *J. Phys. Chem.* **1996**, *100*, 19824−19839; http://comp.chem.umn.edu/amsol/.

of a partial potential energy surface for the pyrrolam isomers and their interconversion through dienolate and allyl anion intermediates (Figure 7). A similar analysis for iminium cation **16** permits the deduction that alcohol **3** and dimer **5** are most likely artifacts of the natural product isolation procedure and not natural agents themselves.

The facile rearrangement of **1** to **9** was not predicted by molecular mechanics calculations based on the relative stabilities of the two double bond isomers. It illustrates the difficulties that small strained cyclic molecules with conjugated functionality can pose for widely used molecular mechanics programs. Although semiempirical methods fared better, they significantly underestimated the stability of pyrrolam A. Only the MP2 model with a moderate degree of electron correlation comes close to matching the experimental data. Strain and conjugation in small rings challenges many commonly used computational tools, and ab initio calculations should be employed to confirm or deny the reliability of molecular mechanics calculations on such molecules.

Experimental Section

1,1-Dimethylethyl Ester 2(*R*)-[(1*Z*)-3-Ethoxy-3-oxo-1-propenyl]-1-pyrrolidinecarboxylate (7).[12] *N*-Boc-pyrrolidine (342 mg, 2.0 mmol) was dissolved in freshly distilled Et_2O (6.0 mL) along with (−)-sparteine (468 mg, 2.0 mmol). The reaction mixture was cooled to −78 °C under an argon atmosphere, and *s*-BuLi (1.25 mL, 2.0 mmol) was added dropwise by syringe. The resultant solution was stirred at −78 °C for 1 h. Then a solution containing CuCN (90 mg, 1.0 mmol) and LiCl (90 mg, 2.0 mmol) in THF (6.0 mL) was added portion-wise by syringe. The mixture was allowed to stir at −78 °C for 30 min before the addition of ethyl (*Z*)-3-iodopropenoate (226 mg, 1.0 mmol). The reaction was allowed to slowly warm to room temperature overnight, diluted with Et_2O (20 mL), and quenched with HCl (5% aqueous, 15 mL). Upon separation of the layers, the organic layer was dried ($MgSO_4$) and concentrated in vacuo to give an oil, which was purified by column chromatography (R_f 0.3, petroleum ether/EtOAc, 90:10, v/v) to afford carbamate **7**[12] as a clear colorless oil (229 mg, 85%).

Ethyl 3-[(2*R*)-2-Pyrrolidinyl]-2-(*Z*)-propenoate Hydrochloride (8). To a solution of pyrrolidinyl carbamate **7** (269 mg, 1.0 mmol) in MeOH (5.0 mL) was added chlorotrimethylsilane (216 mg, 2.0 mmol). The mixture was allowed to stir overnight at room temperature and then concentrated in vacuo to afford a thick oil, which crystallized upon addition of THF to **8** as a white, highly hygroscopic solid (200 mg, 97%): ^{1}H NMR ($CDCl_3$) δ 1.23 (t, J = 7.1 Hz, 3H), 1.70−1.95 (m, 1H), 1.95−2.20 (m, 2H), 2.40−2.60 (m, 1H), 3.25−3.55 (m, 2H), 4.12 (q, J = 7.1 Hz, 2H), 5.11 (br s, 1H), 5.94 (d, J = 11.2 Hz, 1H), 6.68 (m, 1H), 9.78 (br s, 2H); ^{13}C NMR ($CDCl_3$) δ 14.0, 23.6, 31.3, 45.2, 57.6, 60.7, 123.6, 141.6, 165.1.

(*R*)-(−)-Pyrrolam A or (7a*R*)-5,6,7,7a-Tetrahydro-3*H*-pyrrolizin-3-one (1). The HCl salt **8** (620 mg, 3.0 mmol) was dissolved in CH_2Cl_2 (15 mL) and added portionwise at room temperature to a rapidly stirring, biphasic mixture containing saturated aqueous $NaHCO_3$ (10 mL) and CH_2Cl_2 (40 mL). *It is imperative to use a biphasic mixture of methylene chloride and aqueous sodium bicarbonate and to proceed with an inverse addition.* This mixture was allowed to stir for 12 h at room temperature, and then the layers were separated. The organic layer was dried ($MgSO_4$) and concentrated in vacuo to afford (*R*)-(−)-pyrrolam A (**1**) as a clear, light yellow oil (336 mg, 91%): IR(film) 1678 (s) cm^{-1}; ^{1}H NMR ($CDCl_3$) δ 0.95−1.25 (m, 1H), 1.80−2.05 (m, 1H), 2.05−3.00 (m, 2H), 3.10−3.25 (m, 1H), 3.25−3.45 (m, 1H), 4.18 (dd, J = 6.0 Hz, 4.7 Hz, 1H), 5.94 (dd, J = 1.46 Hz, 4.28 Hz, 1H), 7.13 (dd, J = 1.68 Hz, 4.0 Hz, 1H); ^{13}C NMR ($CDCl_3$) δ 28.9, 29.8, 41.7, 67.8, 128.2, 148.8, 175.9; MS *m*/*z* (rel intensity) 123 (61, M^+), 95 (72), 67 (100), 55 (10).

The enantiomeric purity of (*R*)-(−)-pyrrolam A (**1**) was determined by chiral stationary phase HPLC on a CHIRACEL OD column [cellulose tris(3,5-dimethylphenylcarbamate) on silica gel] to be a 90:10 er [hexane/^{i}PrOH, 90:10 (v/v), flow rate = 0.5 mL/min, detection at λ = 254 nm], which compares well with the 90:10 er determined for the starting ester **7**. The (*S*)-enantiomer (minor) eluted first with a retention time of 22.14 min followed by the (*R*)-isomer (major) at 24.64 min. Purification [silica gel chromatography, MeOH/$CHCl_3$ (1:9, v/v)] of the NMR sample (32 mg) of **1** gave a white solid [26.5 mg, mp = 56−58 °C, $[\alpha]_D$ −21.7] comparable to the literature reports [mp = 62 °C, $[\alpha]^{24}_D$ −29.3 (*c* 1.0, $CHCl_3$);[4] mp = 60−62 °C, $[\alpha]_D$ −26.3 (*c* 0.31, $CHCl_3$);[5] mp = 59 °C, $[\alpha]^{24}_D$ −26.3 (*c* 0.8, $CHCl_3$);[7] mp = 61.5 °C, $[\alpha]^{24}_D$ −26.3 (*c* 0.4, $CHCl_3$)[8]].

2,5,6,7-Tetrahydro-3*H*-pyrrolizin-3-one (9). The HCl salt **8** (205 mg, 1.0 mmol) was suspended in THF (5.0 mL) and added to a rapidly stirring, cold (0 °C) solution of lithium hexamethyldisilazide (LiHMDS, 2.0 equiv) in THF (10 mL). After 20 min of stirring, H_2O (10 mL) was added, and the layers were separated. The organic layer was dried ($MgSO_4$) and concentrated in vacuo to afford enamide **9** as a light yellow, clear oil (118 mg, 96%): ^{1}H NMR ($CDCl_3$) δ 2.20−2.40 (m, 2H), 2.45−2.55 (m, 2H), 3.25 (dt, J = 2.7 Hz, 2.9 Hz, 2H), 3.43 (t, J = 6.8 Hz, 2H), 4.79 (t, J = 2.1 Hz, 1H); ^{13}C NMR ($CDCl_3$) δ 23.6, 27.5, 40.2, 43.2, 93.3, 149.2, 174.9.

1,2,5,6-Tetrahydro-3*H*-pyrrolizin-3-one (10).[14] Enamide **9** was left exposed to the laboratory atmosphere for 20 min with only residual traces of solvent (EtOAc) remaining. Concentration in vacuo afforded the isomeric enamide **10** as the major component of a 78:22 mixture of **10**:**9**. A mixture of **1**:**9**:**10** enriched in **10** was also obtained by attempted purification of **9** by column chromatography on basic alumina: ^{1}H NMR ($CDCl_3$) δ 2.50−2.65 (m, 2H), 2.65−2.80 (m, 2H), 2.80−3.00 (m, 2H), 3.58 (t, J = 8.7 Hz, 2H), 4.59 (t, J = 1.9 Hz, 1H); ^{13}C NMR ($CDCl_3$) δ 18.6, 33.6, 34.9, 40.0, 97.4, 147.2, 170.9

Alternative Synthesis of (10). To a suspension of the phosphonium iodide (529 mg, 1.0 mmol, Scheme 2, see Supporting Information for preparation) in anhydrous THF (30 mL) was added potassium *tert*-butoxide (136 mg, 1.2 mmol) at 0 °C. The reaction mixture was stirred at room temperature for 18 h and then refluxed for 3 h. After cooling to room temperature, the mixture was poured into ice−water (50 mL) and extracted with diethyl ether (3 × 20 mL). The combined extracts were dried over anhydrous $MgSO_4$ to give the crude material (100 mg) contaminated with small amounts of Ph_3PO: ^{1}H NMR ($CDCl_3$) δ 2.58 (br s, 2H), 2.77 (br s, 2H), 2.92 (br s, 2H), 3.62 (t, J = 8.6, 2H), 4.55 (s, 1H); ^{13}C NMR ($CDCl_3$) δ 18.7, 33.7, 35.0, 40.1, 97.6, 146.6, 170.9.

Pyrrolam C or (Hexahydro-7a-hydroxy-3*H*-pyrrolizin-3-one (3). Enamide **9** (123 mg, 1 mmol) was dissolved in EtOAc (5 mL), and wet silica gel (500 mg, 400 mesh) was added. The slurry was stirred at room temperature for 12 h and then filtered. Concentration in vacuo followed by chromatography on alumina (R_f = 0.3, 100% EtOAc) afforded pyrrolam C (**3**) as a slightly yellow solid (127 mg, 90%): mp 71−72 °C; IR (film) 3378(br), 2981 (m), 1678 (s) cm^{-1}; ^{1}H NMR ($CDCl_3$) δ 1.52−1.64 (m, 1H), 1.98−2.25 (m, 4H), 2.25−2.42 (m, 2H), 2.92 (dt, J = 17 Hz, 9.6 Hz, 1H), 3.10−3.20 (m, 1H), 3.38 (dt, J = 5 Hz, 3.2 Hz, 1H), 5.00 (s, 1H); ^{13}C NMR ($CDCl_3$) δ 25.6, 33.9, 34.0, 37.8, 40.5, 97.8, 174.9; MS *m*/*z* (rel intensity). Anal. Calcd for $C_7H_{11}NO_2$: C, 59.57; H, 7.80; N, 9.93. Found: C, 59.74; H, 7.84; N, 9.73.

Hexahydro-7a-methoxy-3*H*-pyrrolizin-3-one [Pyrrolam B] (2). Pyrrolam C (**3**) (127 mg, 0.9 mmol) was dissolved in MeOH (5.0 mL), and dry silica gel (500 mg, 400 mesh) was added. The slurry was stirred at room temperature for 12 h and then filtered. Concentration in vacuo afforded a mixture of **3** and pyrrolam B (**2**) as a clear, yellow oil (98 mg): ^{1}H NMR

($CDCl_3$) δ 1.54−1.61 (m, 1H), 2.04−2.17 (m, 3H), 2.20−2.32 (m, 2H), 2.44−2.53 (m, 1H), 2.80−2.89 (m, 1H), 3.06−3.14 (m, 1H), 3.21 (s, 3H), 3.55−3.63 (m, 1H); ^{13}C NMR ($CDCl_3$) δ 25.4, 28.2, 34.7, 37.3, 41.2, 49.8, 101.7, 175.4.

Computational Methods. All ab initio, density functional calculations, as well as geometry optimizations, chemical shift evaluations, and solvation calculations were performed with Gaussian 03.[18] MM3* and MMFF molecular mechanics geometries and energy evaluations using the GBSA continuum solvation method[25] were carried out with MacroModel.[26] AM1, PM3, and MNDO results were obtained with various versions of Spartan[27] as indicated in the footnotes of Table 2. ^{13}C NMR chemical shifts using the MP2 model (Table S-1, Supporting Information) required large memory requirements. As a result, each ^{13}C value was computed individually one job at a time using a mixed basis set, the locally dense basis set method.[28] Thus, the carbon in question was evaluated at the MP2/6-311G* level, whereas the remainder of the molecule was treated at the MP2/3-21G* level.

Acknowledgment. This work was generously supported by the National Institutes of Health (GM-60300-01) and the National Science Foundation (CHE-0132539). Support of the NSF Chemical Instrumentation Program for purchase of a JEOL 500 MHz NMR instrument is gratefully acknowledged (CHE-9700278). We are grateful to Professor Luigi Gomez-Paloma (University of Salerno, Italy) for alerting us to the usefulness of the mPW1PW91 DFT method.

Supporting Information Available: ^1H and ^{13}C NMR spectra for compounds **1**, **9**, **10**, **3**, and the **1** + **9** and the **1** + **9** + **10** mixtures; ^1H NMR spectrum for **9**; chiral HPLC trace for **1**; procedure for preparation of the phosphonium salt used in the synthesis of **10**; and table of experimental and calculated ^{13}C NMR chemical shifts for **1**, **9**, and **10**. This material is available free of charge via the Internet at http://pubs.acs.org.

JO049460R

(25) Still, W. C.; Tempczyk, A.; Hawley, R. C.; Hendrickson, T. *J. Am. Chem. Soc.* **1990**, *112*, 6127−6129.

(26) (a) Mohamadi, F.; Richards, N. G. J.; Guida, W. C.; Liscamp, R.; Lipton, M.; Caufield, C.; Chang, G.; Hendrickson, T.; Still, W. C. *J. Comput. Chem.* **1990**, *11*, 440. (b) Cf. http://www.schrodinger.com/

(27) http://www.wavefun.com/

(28) Chesnut, D. B.; Moore, K. D. *J. Comput. Chem.* **1989**, *10*, 648−659.